

# PUS1 is a novel biomarker for evaluating malignancy of human renal cell carcinoma

Lin Li<sup>1,2,\*</sup>, Chongying Zhu<sup>3,\*</sup>, Shouying Xu<sup>1</sup>, Qiang Xu<sup>1</sup>, Da Xu<sup>2</sup>, Sishun Gan<sup>2</sup>, Xingang Cui<sup>4</sup>, Chao Tang<sup>1</sup>

<sup>1</sup>National Clinical Research Center for Child Health of the Children's Hospital, Zhejiang University School of Medicine, Hangzhou 310052, China

<sup>2</sup>Department of Urology, Third Affiliated Hospital of the Second Military Medical University, Shanghai 201805, China

<sup>3</sup>Department of Obstetrics and Gynecology, Ruijin Hospital, Shanghai Jiaotong University School of Medicine, Shanghai 200025, China

<sup>4</sup>Department of Urology, Xinhua Hospital, School of Medicine, Shanghai Jiaotong University, Shanghai 200092, China

\*Equal contribution

**Correspondence to:** Chao Tang, Xingang Cui; **email:** [chtang@zju.edu.cn](mailto:chtang@zju.edu.cn), [cuxingang@xinhumed.com.cn](mailto:cuxingang@xinhumed.com.cn)

**Keywords:** PUS1, renal cell carcinoma, biomarker, malignancy

**Received:** February 27, 2023

**Accepted:** June 1, 2023

**Published:** June 13, 2023

**Copyright:** © 2023 Li et al. This is an open access article distributed under the terms of the [Creative Commons Attribution License](https://creativecommons.org/licenses/by/3.0/) (CC BY 3.0), which permits unrestricted use, distribution, and reproduction in any medium, provided the original author and source are credited.

## ABSTRACT

Renal cell carcinoma (RCC) is one of the most common malignancies. Despite the rapid development of the oncology research and surgical treatment, the prognosis of RCC has not significantly improved. Thus, exploration of the pathological molecular mechanism and development of new therapeutic targets of RCC are of great importance. Herein, by bioinformatic analysis and *in vitro* cell experiments, we report that, the expression of pseudouridine synthase 1 (PUS1), belonging to the family of PUS enzymes that participate in RNA modifications, is closely associated with RCC progression. In addition, the upregulated PUS1 expression results in the elevated RCC cancer cell viability, migration, invasion and colony formation ability, whereas the decreased PUS1 expression exerts the opposite effects on RCC cells. Thus, our findings show the potential role of PUS1 in RCC cells, providing with evidence that PUS1 is involved in RCC progression, which may help contribute to RCC diagnosis and intervention in clinic.

## INTRODUCTION

As shown by the latest data of cancer from the United States, renal cell carcinoma (RCC), which is recognized as the most common malignancy of the genitourinary system, ranks the sixth most common cancer in men, with 65000 new cases and 15000 deaths per year [1]. Despite the rapid development of the research in cancer and clinical surgical treatment, the prognosis of RCC has not significantly improved in clinic at present. Due to the shortage of effective molecular bio-markers for the RCC treatment, plenty of

patients with renal cancer consequently develop to advanced stage [2, 3]. In recent years, although targeted agents have been applied, showing the function in prolonging the survival and prognosis particularly in patients with tumor metastases, the median survival of patients remains less than three years [4]. Moreover, drug resistance and economic burden have become the two major problems in clinical practice [5]. Thus, exploration of the pathological molecular mechanism and development of promising therapeutic targets for RCC are of great importance for better treatment of RCC.

Accumulating evidence has suggested that RNA modifications play a pivotal role in epigenetic regulation of gene expression in sustaining physiological functions, and dysregulation of RNA modifications gives rise to various diseases, including cancer [6–8]. As an isomer of uridine, pseudouridine is found to be the most abundant RNA modification and is recognized to be the fifth RNA nucleotide [9, 10]. Previous studies have demonstrated that the isomerization process of uridine to pseudouridine can be triggered by either of the two following mechanisms: (1) by a small nucleolar RNA-dependent mechanism where the box H/ACA ribonucleoproteins are incorporated; (2) by an RNA-independent mechanism that requires the stand-alone pseudouridine synthase (PUS) enzymes [11, 12]. To date, the PUS enzymes can be divided into six families, including the TruA, TruB, TruD, RsuA, RluA and Pus10 families [13]. While RNA pseudouridylation has been suggested to be associated with human physiological functions and diseases [14, 15], the biological regulation of PUS remains largely unknown.

As an important member belonging to the pseudouridine synthase family, PUS1 is found to participate in regulating the pseudouridylation modification of almost all kinds of RNAs, including tRNAs, ncRNAs, mRNAs, snoRNAs, and snRNAs [16, 17]. Despite its role in various diseases such as myopathy, lactic acidosis and sideroblastic anaemia (MLASA) syndrome [18, 19] where *PUS1* gene is mutated, recent studies additionally elucidated the versatile role of PUS1 in cancer. In a latest report, PUS1 expression was shown to be positively correlated with triple-negative breast cancer (TNBC) status and tumor grade, and thereby can be potentially applied for predicting poor outcomes and triple-negative status in breast cancer [16].

In this study, by bioinformatic analysis, experiments *in vitro* and clinical RCC samples, we report herein that PUS1 expression was closely associated with RCC progression and the upregulated PUS1 expression results in the elevated RCC cancer cell viability and mobility, providing with the evidence that PUS might be a promising treatment target for RCC therapy.

## MATERIALS AND METHODS

### Data collection

The gene expression, mRNA sequencing (mRNA) expression and clinical information of 532 kidney renal clear cell carcinoma samples were retrieved from the Cancer Genome Atlas (TCGA) database (<https://portal.gdc.cancer.gov/>). The normal kidney

composed of 72 TCGA samples and 89 GTEx database. GTEx datasets are available at the GTEx data portal (<https://www.gtexportal.org/home/datasets>) for the current release (V8). The four GEO clear cell renal cancer cohorts (GSE15641, GSE17818, GSE17895, and GSE40435) were obtained from the Gene-Expression Omnibus (GEO) (<https://www.ncbi.nlm.nih.gov/geo/>) as MINiML files. In GSE15641, 23 control samples and 32 clear cell renal samples were enrolled; in GSE17818, 13 normal patients and 103 renal clear cell carcinoma patients; in GSE17895, the data contained 22 health renal samples and 138 patients; and the GSE40435 dataset had included 101 health kidney and 101 kidney clear cell carcinoma.

### Biological data processing

For 14 TCGA cancer types with over ten paired tumor and normal samples (THCA, KIRP, BLCA, LIHC, HNSC, BRCA, LUAD, PRAD, ESCA, KICH, LUSC, KIRC, STAD, COAD), we performed GSCA differential expression analysis using normalized and batch corrected RSEM mRNA expression. We calculated the fold change by dividing the mean of the tumor by the mean of the normal, and our *p*-value is estimated by a *t*-test and then adjusted by the Fisher's exact test. The data from GEO contain the platform, samples and GSE records. The microarray data were normalized by the R (version 3.4.1) preprocess core package named "Normalize. Quantiles" following the  $\log_2$  transformation. Gene symbols were generated from probes based on the annotation information in the normalized data. The Kaplan-Meier (KM) survival analysis with log-rank test was applied for comparing the survival difference between the above two groups. For KM curves, *p*-values and hazard ratio (HR) with 95% confidence interval (CI) were generated by log-rank tests and univariate Cox proportional hazards regression as described previously [20]. All analytical methods above and R packages were performed using R software.  $P < 0.05$  was considered as statistically significant.

### Enrichment analysis

After using limma package to study the differential expression of the mRNA from TCGA, a functional enrichment analysis was conducted to further confirm the underlying function of potential targets. The Gene Ontology (GO) analysis and Kyoto Encyclopedia of Genes and Genomes (KEGG) analysis were performed to annotate genes with functions. The ClusterProfiler package in R was used to analyze the GO function and enrich the KEGG pathway. The R software ggplot2 package was employed to draw boxplot, and the pheatmap package was employed to draw heatmap.

## Construction and assessment of the nomogram

We further conducted Univariate and multivariate cox regression analysis to identify the proper terms to build the nomogram as described previously [21]. The forest showed the *P* value, HR and 95% CI of PUS1, age, gender, TNM stage and grade by “forestplot” R package. Multivariate cox proportional hazards analysis was used to develop a nomogram to predict 1-year, 3-year and 5-year overall recurrence. Based on the nomogram’s points associated with each risk factor, an individual patient’s risk of recurrence can be calculated by “RMS” R package.

## The renal cancer cell line analysis

The mRNA expression matrix of 33 renal cancer cell lines was downloaded from the Cancer Cell Line Encyclopedia (CCLE) portal (<https://www.broadinstitute.org/ccle>) and the analysis was generated by the R ggplot2 package.

## Cell culture

Human embryonic kidney 293T (HEK293T) cells and human RCC cell lines, including Caki-1, 786-O, ACHN, OSRC2, A498, Caki-2 and 769P cells, were purchased from the Chinese Academy of Sciences (Shanghai, China). HEK293T cells were maintained in high glucose DMEM (Hyclone, Logan, UT, USA) supplemented with 10% (v/v) fetal bovine serum (FBS, Life Technologies, Inc., Grand Island, NY). ACHN cells were cultured in MEM medium (Hyclone, USA) supplemented with 10% FBS, and Caki-1, Caki-2, 786-O, OSRC2, A498 and 769P cells were all incubated in RPMI-1640 medium (Hyclone, USA) containing 10% FBS as described previously [22]. All the cells were grown as a monolayer on plastic cell culture dishes at 37°C in 5% CO<sub>2</sub>.

## Antibodies

Anti-PUS1 (#db3219) antibody was from DiagBio (Hangzhou, China) and HA-tag (AF2305) antibody was obtained from Beyotime Biotechnology (Shanghai, China). Glyceraldehyde-3-phosphate dehydrogenase (GAPDH, sc-32233) antibody was purchased from Santa Cruz Biotechnology (Santa Cruz, CA, USA).

## Plasmids, viruses and infections

The PUS1 lentiviral expression vector, pLV3-CMV-PUS1-3×HA-CopGFP-Puro, was constructed by Mr. Lin Li, and the pLV3-CMV-3×HA-CopGFP-Puro empty vector was used as a control. The lentiviral shRNA-expressing vector, pLKO.1-EGFP-PUS1-

shRNA-puro, was constructed by Dr. Shouying Xu, and the pLKO.1-EGFP-puro empty vector carrying a scrambled sequence was used as a control. Lentiviruses were generated by co-transfecting the HEK293T packaging cells with lentiviral plasmids and packaging plasmids (PsPAX and PMD2.0G) as described previously [23]. The lentiviruses-containing supernatants with the titers greater than  $1 \times 10^6$  cfu/ml were used for subsequent infection in the presence of 8 µg/ml polybrene (Sigma-Aldrich, St. Louis, MO, USA). After infection, cells were selected with puromycin at a dose of 2 µg/mL for seven days, and then the cells were cultured with puromycin at a low dose and were subsequently prepared for following experiments.

## Western blotting

Total protein from human RCC Caki-1, 786-O, ACHN, OSRC2, A498, Caki-2 and 769P cells were obtained using RIPA lysis buffer (Beyotime, Shanghai, China), and protein concentrations were determined by standard Bradford assay with a commercial kit (Beyotime, Shanghai, China), followed by western blotting as described previously [24–26]. Briefly, 50 µg of total protein was subjected to SDS-PAGE followed by a transfer onto polyvinylidene fluoride (PVDF) membranes (Millipore, Bedford, MA, USA). Then, membranes were incubated with different primary antibodies at 4°C overnight, and were further incubated with corresponding secondary antibodies (Beyotime, Shanghai, China) the next day. Immunosignals were developed by using the Enhanced Chemiluminescence System.

## Cell counting kit-8 (CCK-8) assays

CCK-8 assays were conducted as described previously [26, 27]. Briefly, cells were seeded into 96-well plates and were infected with PUS1-expressing lentiviruses, control lentiviruses, PUS1-shRNA-expressing lentiviruses, or lentiviruses with scrambled shRNA. After continued culture for 48 h, cells in each well were subjected to 20 µl CCK-8 solution (Beyotime, Shanghai, China) and were cultured for 2 h. Cell viability was subsequently examined by measuring the absorbance at 450 nm *via* a multi-mode plate reader (Bio-Tek Instruments, Hopkinton, MA, USA).

## Wound healing assays

Wound healing assays were performed as previously described [28]. Briefly,  $4 \times 10^5$  cells were cultured in six-well plates and were infected with PUS1-expressing lentiviruses, control lentiviruses, PUS1-shRNA-expressing lentiviruses, or lentiviruses with scrambled shRNA, and were cultured for 24 h. Then,

the cells were subjected to serum starvation for 12 h. After that, cells were rinsed with medium and the confluent cell layer was scratched with a sterile tip to generate an artificial wound. After 12 h, migrated cells were observed by microscopy and the distance between the edges of the “wound” was consequently analyzed.

### Matrigel invasion assays

Cell invasive capacity was determined by using Matrigel (BD Biosciences, Franklin Lakes, NJ, USA) coated Transwell inserts (6.5  $\mu$ m, Costar, Cambridge, MA, USA) containing polycarbonate filters with pores (8  $\mu$ m) as detailed previously [28]. Briefly, a mixture of Matrigel and culture medium at the volume proportion of 1:2 at 50  $\mu$ l was enclosed by each membrane in Transwell inserts, respectively. After infection and culture for 48 h,  $2 \times 10^5$  cells in a total volume of 200  $\mu$ l of serum-free medium were added in the upper chamber, while 500  $\mu$ l of culture medium with 10% FBS was loaded to the corresponding lower well. After culture for another 24 h, non-invaded cells were gently removed from the upper surface of the filter, and the cells that had moved through the filter and stayed at the bottom of the Transwell membrane were fixed in ice-cold methanol and were then stained with 0.2% crystal violet-PBS solution (m/v) for 10 min at room temperature. Numbers of the invasive cells from the bottom of the Transwell membrane in six randomly selected fields were counted in each experiment, and the invasive cells were consequently observed and counted using a light microscope.

### Colony formation assays

Colony formation assay was performed as previously described [29]. Briefly, cells were infected with PUS1-expressing lentiviruses, control lentiviruses, PUS1-shRNA-expressing lentiviruses, or lentiviruses with scrambled shRNA. At 24 h after infection, cells were seeded in 6-well plates at a density of 1000 cells/well in 2 ml culture medium. After growing for two weeks, colonies were stained with 0.5% crystal violet solution at room temperature, and colonies were subsequently counted, photographed and statistically analyzed.

### RCC tissue sample obtainment

A total of 10 pairs of RCC tissues and adjacent non-tumor tissues were collected from patients undergoing surgery at the Third Affiliated Hospital of the Second Military Medical University from 2021 to 2022. For inclusive criteria, patients didn't receive any chemotherapy or radiotherapy before operation. All the tumor tissues and paired adjacent non-tumor tissues

were identified by pathologists. A protocol associated with this study was approved by the Third Affiliated Hospital of the Second Military Medical University institutional review board, and informed consent was obtained from each patient.

### Statistical analysis

Data were expressed as mean  $\pm$  SD, and were analyzed by one-way ANOVA and Tukey-Kramer multiple comparison test (SPSS 13.0J software; SPSS, Inc., Chicago, IL).  $P < 0.05$  and  $p < 0.01$  were considered with statistical significance.

### Availability of data and materials

All data generated or analyzed during this study are included in this published article.

### Consent for publication

The author declares that all work described here has not been published before and that its publication has been approved by all co-authors.

## RESULTS

### The expression of PUS1 is increased in renal cancer

Firstly, we investigated the expression of pseudo-uridylylate synthases family in pan-cancer using The Cancer Genome Atlas (TCGA) database online. Totally 14 TCGA cancer types were enrolled, including thyroid carcinoma (THCA), kidney renal papillary cell carcinoma (KIRP), bladder urothelial carcinoma (BLCA), liver hepatocellular carcinoma (LIHC), head and neck squamous cell carcinoma (HNSC), breast invasive carcinoma (BRCA), lung adenocarcinoma (LUAD), prostate adenocarcinoma (PRAD), esophageal carcinoma (ESCA), kidney chromophobe (KICH), lung squamous cell carcinoma (LUSC), kidney renal clear cell carcinoma (KIRC), stomach adenocarcinoma (STAD) and colon adenocarcinoma (COAD), which have over ten paired tumor and normal samples, correspondingly. According to our findings, the expression of *PUS1*, *PUS7*, *DKC1* and *RPUSD1* is highly expressed in most cancer types, and among those genes, the expression of *PUS1*, *PUS7* and *RPUSD1* is markedly upregulated in renal cancers, including KICH, KIRC and KIRP (Figure 1A, 1B). In addition, we also examined the *PUS1* gene expression in four Gene Expression Omnibus (GEO) datasets, including GSE15641, GSE17878, GSE17895 and GSE40435. As expected, the results exhibited the increase of *PUS1* expression in renal cancer (Figure 1C–1F). Consistently, the overall survival of KIRC between high

levels of *PUS1* and low levels of *PUS1* revealed statistical significance (Figure 1G), indicating the higher expression of *PUS1* may be associated with prognosis of renal cancer.

### The differential mRNA expression between clear cell renal cancer and normal tissue

We next analyzed the KIRC data from TCGA database and conducted the heatmap to compare the differentially

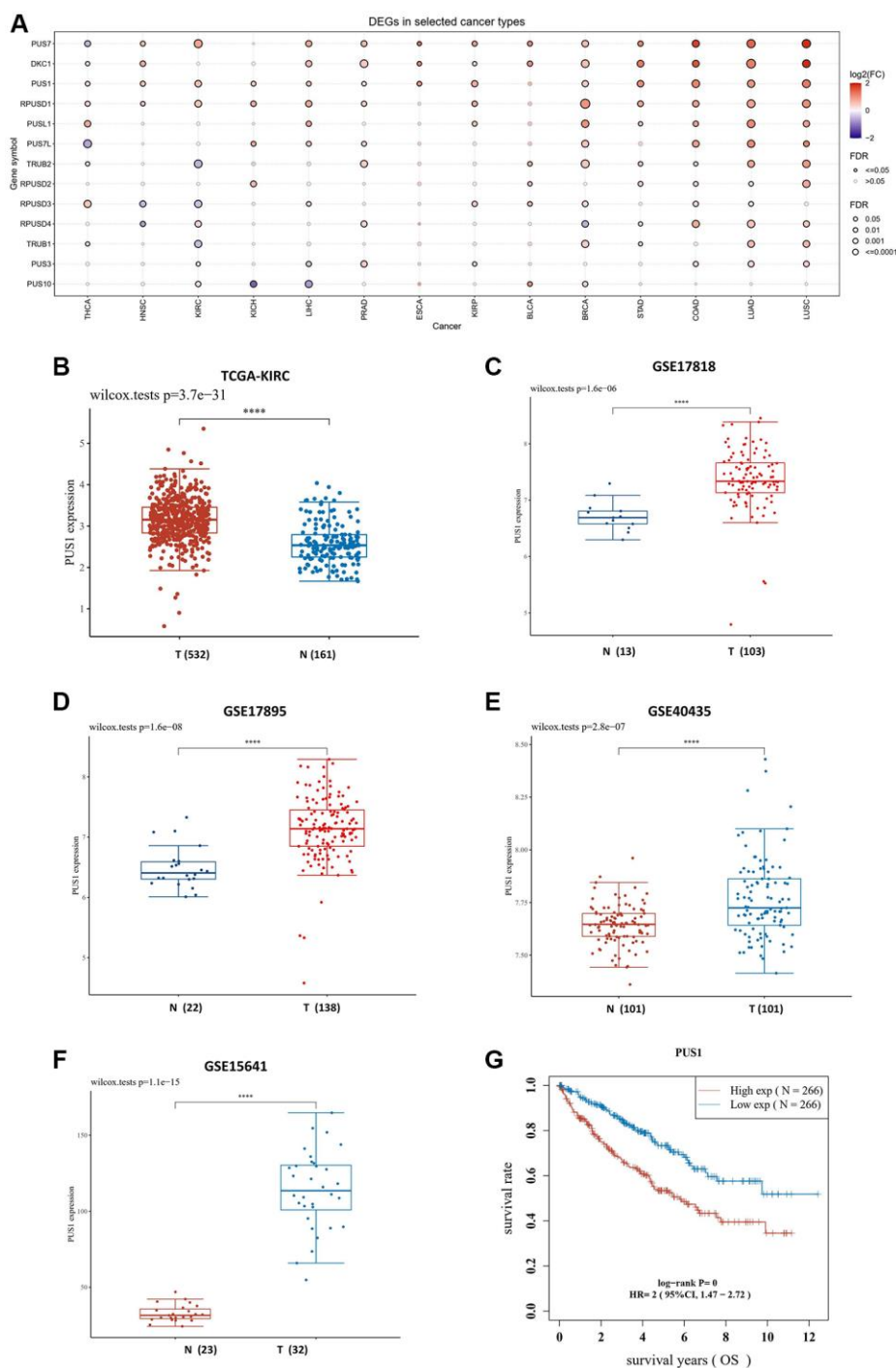


**Figure 1. The expression of PUS1 is increased in renal cancer.** (A) Expression of PUS family gene in pan-cancer. The color of bubbles represents the difference in expression of PUS family genes between tumor tissues and paired normal para-cancer tissues. Red: up-regulated expression in tumor tissues; blue, down-regulated expression in tumor tissue; bubble size indicates significant difference. (B) The expression of PUS1 in KIRC. Red: tumor tissue; blue: paired para-cancer normal tissue. (C–F) The PUS1 gene expression in four GEO datasets, including GSE17818 (C), GSE17895 (D), GSE40435 (E) and GSE15641 (F). (G) The overall survival (OS) of PUS1 in KIRC. Red: high expression group of PUS1; blue: low expression group of PUS1.

expressed genes (DEGs) (Figure 2A). The volcano plots of DEGs were visualized between the cancer and normal tissues, and the value of  $\log_2(\text{fold changes})$  above 1.2 or below  $-1.2$  was defined as the threshold for the differential mRNA expression (Figure 2B).

In total, 9708 DEGs were picked up ultimately, with 7324 up-regulated and 2384 down-regulated (table not shown). Noticeably, the results showed that the expression of genes, including *PUS1*, *PUS7L*, *RPUSD2*, *PUS10*, *RPUSD4*, *TRUB1*, and *DKC1*, was increased,

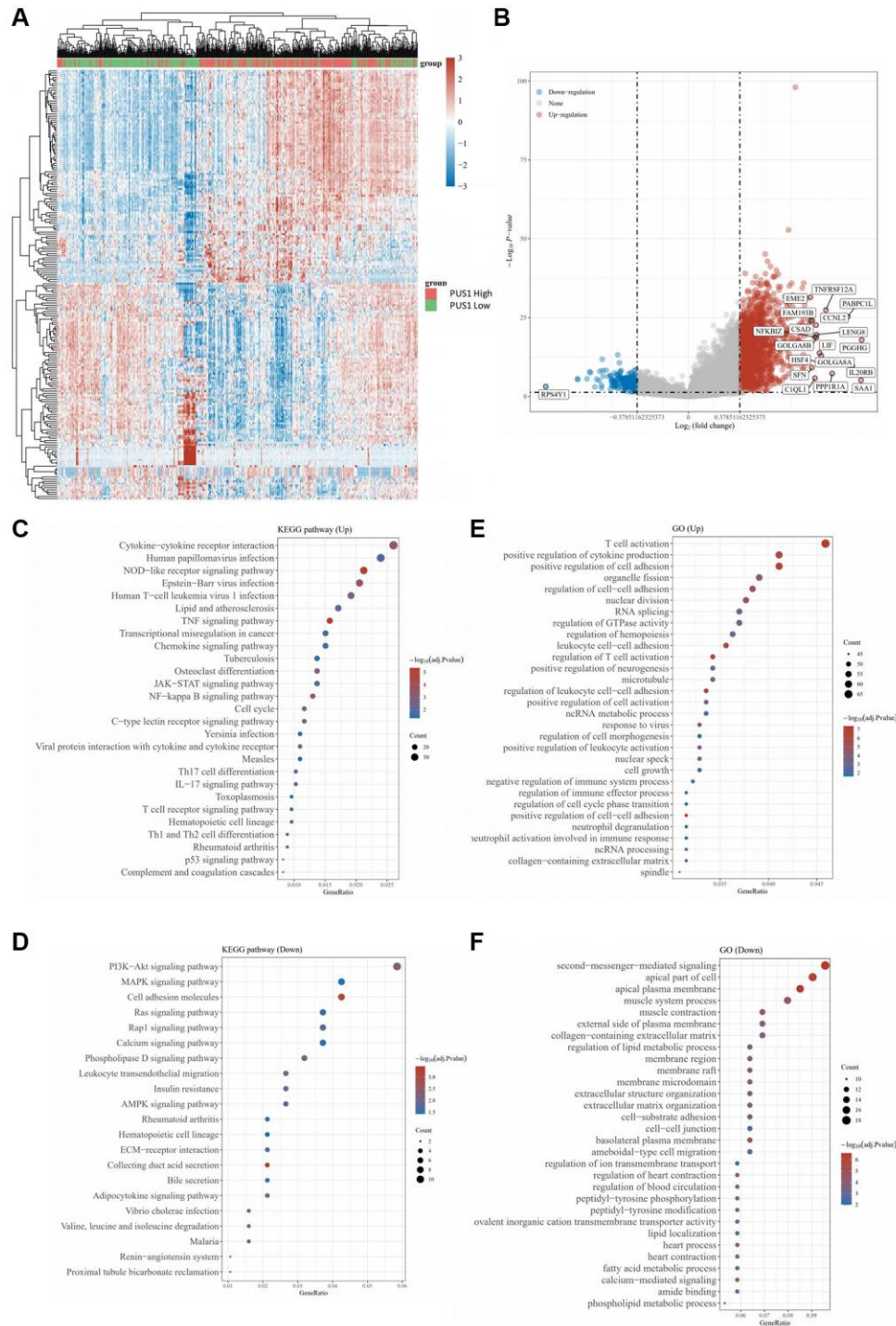


**Figure 2. The differential mRNA expression between clear cell renal cancer and normal tissue.** (A) Heatmap color indicates the differentially expressed genes (DEGs) by analyzing the KIRC data from TCGA database. (B) The volcano plots of DEGs in (A) were visualized. (C, D) GO analysis for enrichment of upregulated (C) and downregulated (D) signaling pathways significantly associated with PUS1 expression in KIRC. (E, F) KEGG analysis for enrichment of upregulated (E) and downregulated (F) signaling pathways significantly associated with PUS1 expression in KIRC.

while conversely, the expression of some genes was decreased, such as *PUSL1* (Figure 2B). To uncover the potential biological processes involved, we next performed the Gene Ontology (GO) analysis and obtained the enrichment for several cancer pathways of DEGs, which particularly focused on cell-cell adhesion and cytokine production, and intriguingly, results also suggested that pathways on immune related activity in T-cell activation were involved (Figure 2C, 2D). Similarly, we further conducted the Kyoto Encyclopedia of Genes and Genomes (KEGG) pathway enrichment analysis with the figure portraying several notable signal pathways, which included PD-1 checkpoint, PD-L1 expression and cell cycle (Figure 2E, 2F).

### Construction of a predictive nomogram

Considering a vital risk of *PUS1* for renal cancer patients, we further developed a clinically predictive

model that was workable and may contribute to estimating the prognosis of renal cancer in clinic. We initially calculated the univariate and multivariate analysis of overall survival (OS) rate, including the expression of genes belonging to the PUS family (*PUS1*, *PUS3*, *PUS7*, *PUS10*, *PUS7L*, *PUSL1*), patients' age, gender, race and Tumor Node Metastasis (TNM)-stage, and set grade as co-variate (Figure 3A, 3B). Intriguingly, our results provided a strong evidence that, similar as TNM-stage and tumor grade, *PUS1* could be a potentially high risk for renal cancer, with a univariate cox regression of (HR 2.46131, 95% CI = 1.81506–3.33766,  $P < 0.0001$ ) and a multivariate cox regression of (HR 1.9173, 95% CI = 1.28641–2.8576,  $P = 0.00139$ ), which had already been accepted as predictive standards for renal cancer prognosis (Figure 3C). Next, we generated a nomogram for 1-year, 3-year, and 5-year renal clear cancer patients OS rate model in the discovery group. The elements of the model

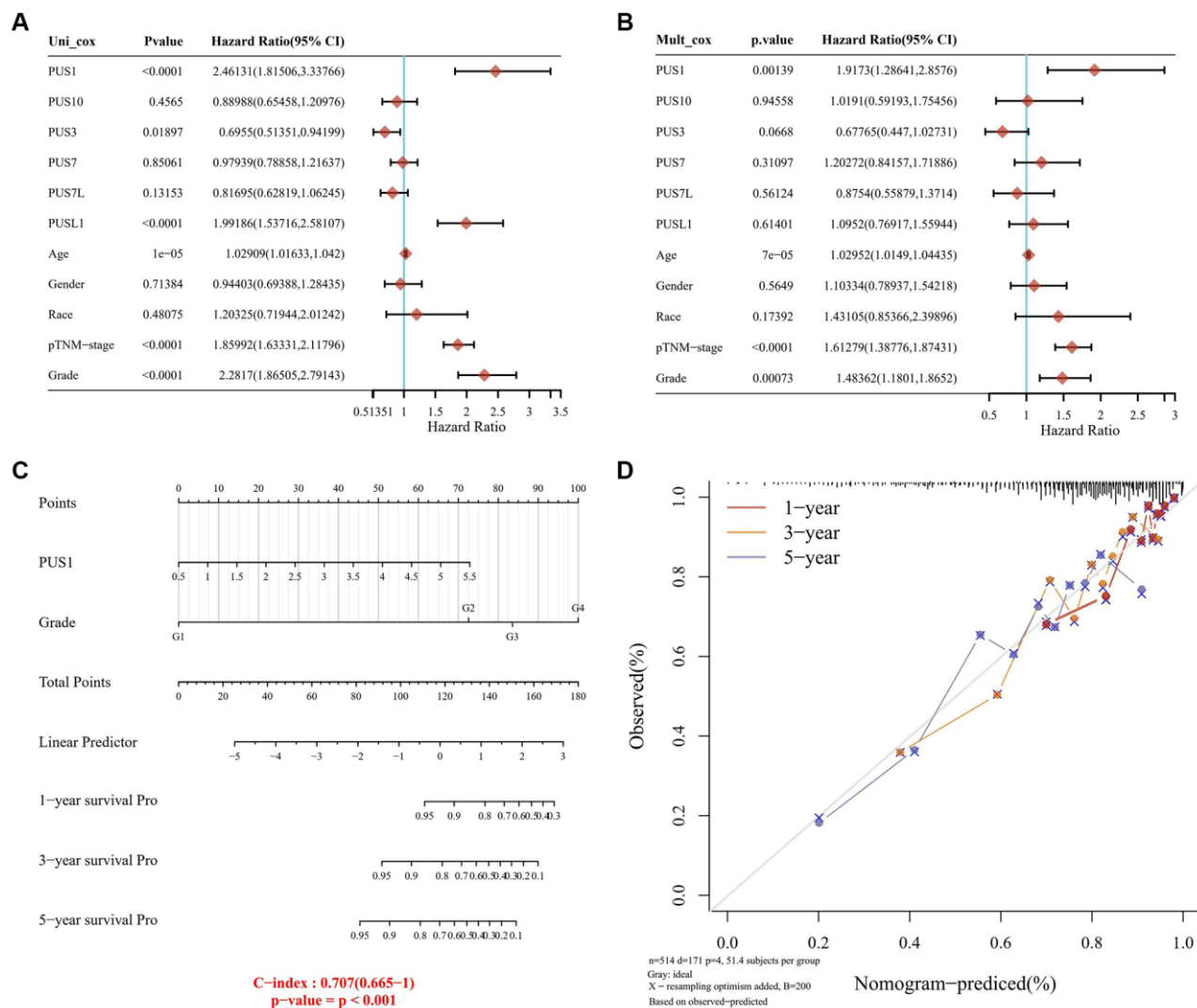


**Figure 3. Construction of a predictive nomogram.** (A, B) Univariate (A) and multivariate (B) Cox regression analyses were performed in renal cancer. (C) The nomogram gives 1-, 3- and 5-year overall survival in renal cancer. (D) The survival time of renal cancer dataset is displayed.

contained tumor grade and *PUS1* expression, with the nomogram showing a promising concordance with 1-year, 3-year, and 5-year OS (Figure 3D).

### Expression levels of *PUS1* are associated with RCC cell malignancy

To figure out whether dysregulation of *PUS1* contributes to RCC progression, we examined the *PUS1* protein expression in seven different RCC cell lines, including BCaki-1, 786-O, OSRC2, ACHN, 769P, A498 and Caki-2. Our results revealed that the expression of *PUS1* in 786-O, OSRC2, ACHN cells was higher than other cell lines (Figure 4A), and the expression was particularly low in A498 cells (Figure 4A), which was consistent with the data of the renal cancer cell line analysis from the CCLE portal (Supplementary Figure 1). In addition, the mRNA expression of *PUS1* was significantly increased in collected RCC tissues compared to that of paired normal tissues, reinforcing the notion that *PUS1* may accelerate RCC progression (Figure 4B).

We next cloned human *PUS1* coding DNA sequence (CDS) sequence and inserted it into the lentivirus vector with 3×HA tags to obtain the pLV3-CMV-*PUS1*-3×HA-CopGFP-Puro plasmid and generated 3×HA-*PUS1* lentiviruses (*PUS1*-LV), whose expression in A498 cells was determined by western blot of detecting *PUS1* and HA tag, respectively (Figure 4C). Meanwhile, we constructed the pLKO.1-EGFP-puro vector containing shRNA sequences targeting *PUS1* to inhibit endogenous *PUS1* expression and generated *PUS1*-shRNA lentiviruses (*PUS1*-shRNA-LV) that significantly suppressed *PUS1* protein expression in ACHN cells (Figure 4D). Infection of *PUS1*-LV significantly potentiated viability in a time dependent-manner, promoted migration, enhanced invasion, and increased colony numbers in A498 cells (Figure 4E, G–4J, 4O, 4P). Conversely, infection of *PUS1*-shRNA-LV resulted in the opposite effects in ACHN cells, including lowered viability at different time points, particularly at 48 h, 72 h and 96 h, down-regulated migration, suppressed invasive capability, and decreased colony numbers (Figure 4F, 4K–4N, 4Q, 4R). In consistence with the migration and invasion data, the expression of epithelial-mesenchymal transition (EMT)-related markers was altered simultaneously. Noticeably, overexpression of *PUS1* by *PUS1*-LV decreased E-Cadherin protein expression but increased Vimentin protein levels in A498 cells (Figure 4S), whereas silencing of *PUS1* by *PUS1*-shRNA-LV induced E-Cadherin expression but repressed Vimentin protein levels in ACHN cells contrarily (Figure 4T), suggesting *PUS1* expression levels were associated with RCC cell mobility and metastasis. These results, which were in

agreement with our bioinformatic analysis of the RNA sequencing data, prove that, *PUS1* participates in RCC progression, indicating that *PUS1* might have potential predictive value for prognosis of RCC in clinic.

## DISCUSSION

In our study, we found that RCC tissues showed the higher expression of *PUS1* than that in normal tissues. As expected, bioinformatic analysis data revealed that the higher expression levels of *PUS1* were correlated with higher tumor grade as well as poor prognosis of patients with RCC. Moreover, according to *in vitro* RNA sequencing analysis data, up-regulation of *PUS1* expression affected a range of cancer related pathways. Consistently, by overexpression of *PUS1* and knockdown of *PUS1* in RCC cells *in vitro*, we showed that *PUS1* expression was significantly associated with cancer cell malignancy, including cell viability, migration, invasion and colony formation ability.

RNA modifications play a vital role in regulating RNA functions and in controlling gene expression. As an important component of translation machinery, transfer RNA (tRNA) is processed and matured with various types of modifications [30]. Among which, pseudouridine is found to be the most abundant modification in RNA, which has been detected in almost all RNA species, but the biological functions of pseudouridine modification in human physiology and diseases remain largely unknown [31]. Previous studies have shown that urinary pseudouridine nucleoside levels are obviously higher in patients with cancer, providing with the possibility that urinary pseudouridine levels may potentially be used as a tumor bio-marker in clinic [32, 33]. Nevertheless, the clues for a direct function of pseudouridine modification and for the various PUS enzymes in carcinogenesis have not been obtained, despite a recent study indicating a potential role for *PUS7* in myelodysplastic syndromes [15]. In the study presented here, we have demonstrated a direct role of *PUS1* in RCC tumorigenesis. Particularly, we have proved that *PUS1* regulates the growth and movement of RCC cells, providing with direct evidence for PUS in modulating urinary tumorigenesis.

Given that high expression of *PUS1* is correlated with poor prognosis in RCC, we therefore hypothesized that *PUS1* could be an oncogene in RCC. As expected, both KEGG pathway analysis and GO bioinformatic analysis indicate that the altered expression of *PUS1* is related to multiple pathways, including cancer pathways and cell function progressions, such as cell proliferation, cell growth, cell movement, cell death and cell differentiation. Consistently, our data of *in vitro* experiments in RCC cell lines demonstrated that *PUS1*



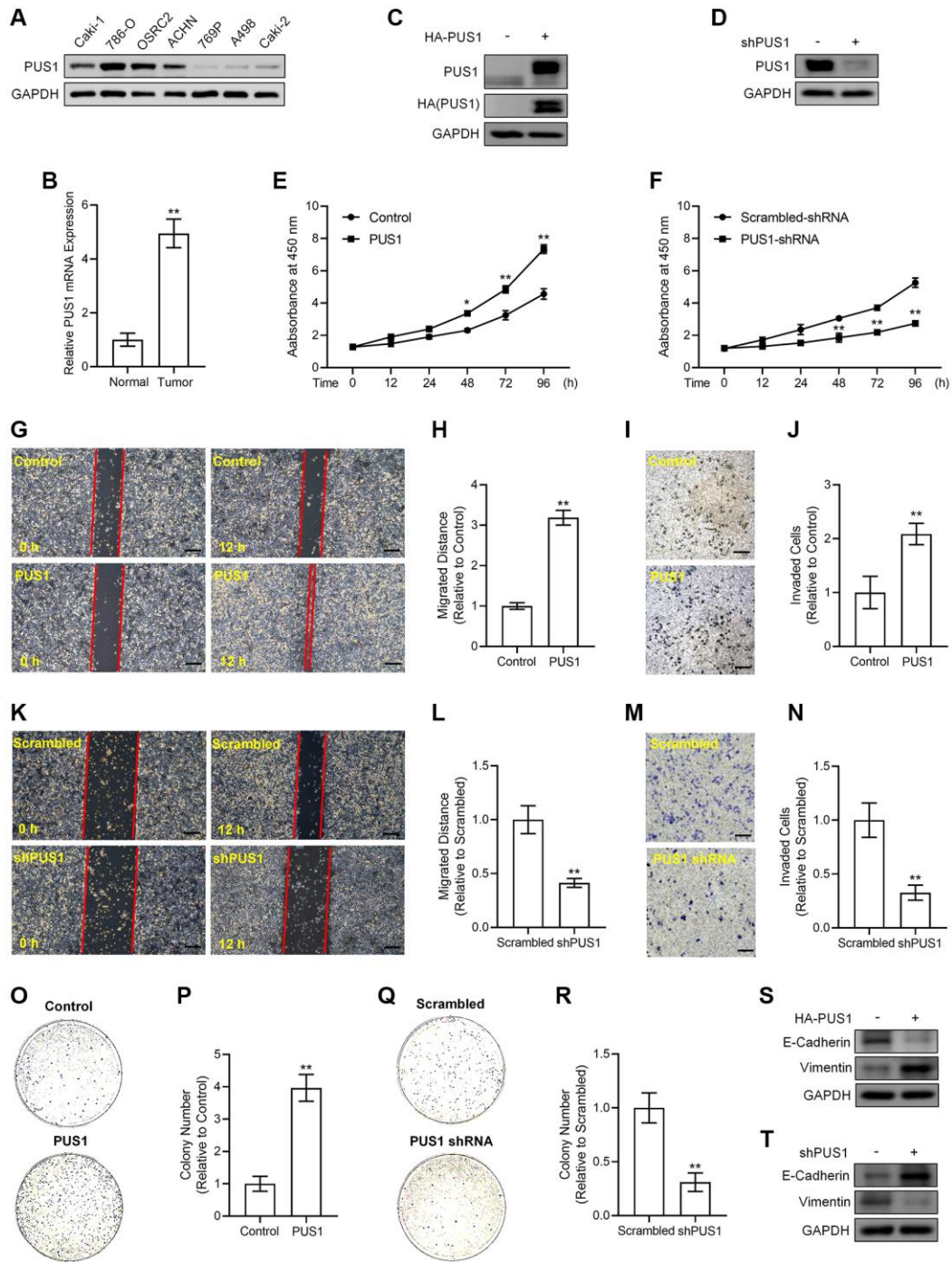


**Figure 4. Alterations in PUS1 expression affect A498 cell and ACHN cell viability, migration, invasion, colony formation, and the expression of E-Cadherin and Vimentin.** (A) The protein expression of PUS1 in different RCC cell lines. (B) The mRNA expression levels of *PUS1* in cancer tissues and adjacent normal epithelial tissues from patients with RCC.  $N = 10$ . (C) A498 cells are infected with PUS1-LV and PUS1 expression was detected by western blot. (D) ACHN cells are infected with PUS1-shRNA-LV and PUS1 expression was detected by western blot. (E) A498 cells are infected with PUS1-LV and cell viability was measured. (F) ACHN cells are infected with PUS1-shRNA-LV and cell viability was measured. (G) A498 cells are infected with PUS1-LV and cell migration was determined by wound healing assay. (H) Quantitative statistics of (G). (I) A498 cells are infected with PUS1-LV and cell invasion was detected by matrigel-transwell assay. (J) Quantitative statistics of (I). (K) ACHN cells are infected with PUS1-shRNA-LV and cell migration was determined by wound healing assay. (L) Quantitative statistics of (K). (M) ACHN cells are infected with PUS1-shRNA-LV and cell invasion was detected by matrigel-transwell assay. (N) Quantitative statistics of (M). (O) A498 cells are infected with PUS1-LV and cell colony formation was performed. (P) Quantitative statistics of (O). (Q) ACHN cells are infected with PUS1-shRNA-LV and cell colony formation was performed. (R) Quantitative statistics of (Q). (S) Protein levels of E-Cadherin and Vimentin in A498 cells infected with PUS1-LV. (T) Protein levels of E-Cadherin and Vimentin in ACHN cells infected with PUS1-shRNA-LV. SD, error bar; \*\* $p < 0.01$ ; \* $p < 0.05$ .

acts as a key mediator in RCC cell biological actions. Considering the RNA-sequencing data showing the downstream cell pathways and genes that are possibly regulated by PUS1, future work is in need to elucidate the molecular mechanisms underlying PUS1 facilitating RCC progression and to figure out the possible function of PUS1 in RCC tumorigenesis in clinic.

Studies on the family of *PUS* gene in cancer are quite few. Despite previous publications showing that PUS7 was correlated with glioblastoma [31], colorectal cancer [34] and ovarian cancer [35], a recent study by Fang et al. reported that PUS1 was overexpressed in breast tumors compared with paired normal tissues, and PUS1 expression was positively correlated with triple-negative breast cancer status and tumor grade [16]. Consistent with their results showing that silencing of PUS1 significantly suppressed breast tumor proliferation and invasion, our data further made a complement for PUS1 function in tumor, providing with evidence that PUS1 would be a potential diagnose marker for cancers, including RCC. Owing to the rapid growth of our better understanding on epitranscriptomes in physiology and diseases, researches on therapeutic strategies targeting the epitranscriptomic machineries are evolving [36]. Thus, designing and developing novel inhibitors for pseudouridine synthases such as PUS1 may contribute to pseudouridine-targeting therapeutic development.

In conclusion, our findings showing the potential role of PUS1 in RCC cells provide with evidence that PUS1 is involved in RCC progression, which may help contribute to RCC diagnosis and intervention in clinic.

## AUTHOR CONTRIBUTIONS

L. Li, C. Zhu and C. Tang performed the experiments. S. Xu, Q. Xu, D. Xu and S. Gan collected the bioinformatic data and analyzed the data. X. Cui analyzed the data and edited the manuscript text. C. Tang designed the study and wrote the manuscript text. All the authors reviewed the manuscript.

## CONFLICTS OF INTEREST

The authors declare no conflicts of interest related to this study.

## ETHICAL STATEMENT AND CONSENT

The present study was approved by the ethics committee of Third Affiliated Hospital of the Second Military Medical University. Written informed consent was obtained from all patients and conducted following the Declaration of Helsinki.

## FUNDING

This work was supported by Foundation for The Top-Notch Youth Talent Cultivation Project of Independent Design Project of National Clinical Research Center for Child Health (No. Q21A0006) and National Natural Science Foundation of China (No. 31801207) to C. Tang, and by National Natural Science Foundation of China (No. 81974391, 82072806), Leading health talents of Shanghai Municipal Health Commission (2022LJ002), Hospital Funded Clinical Research, Xin Hua Hospital Affiliated to Shanghai Jiao Tong University School of Medicine (21XHDB06) to X. Cui.

## REFERENCES

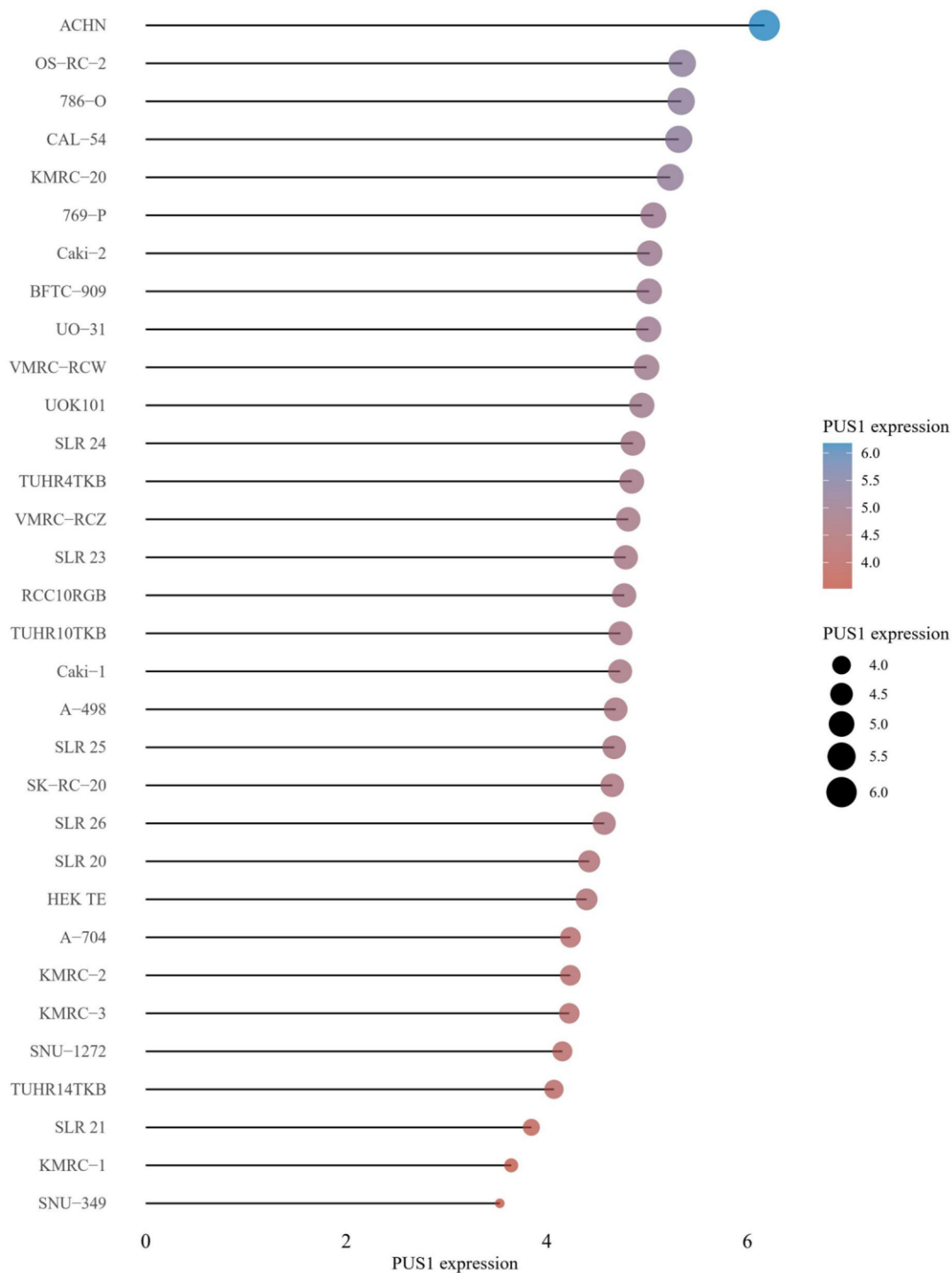
1. Siegel RL, Miller KD, Jemal A. Cancer statistics, 2019. *CA Cancer J Clin.* 2019; 69:7–34. <https://doi.org/10.3322/caac.21551> PMID:[30620402](https://pubmed.ncbi.nlm.nih.gov/30620402/)
2. Escudier B, Porta C, Schmidinger M, Rioux-Leclercq N, Bex A, Khoo V, Grünwald V, Gillessen S, Horwich A, and ESMO Guidelines Committee. Renal cell carcinoma: ESMO Clinical Practice Guidelines for diagnosis, treatment and follow-up†. *Ann Oncol.* 2019; 30:706–20. <https://doi.org/10.1093/annonc/mdz056> PMID:[30788497](https://pubmed.ncbi.nlm.nih.gov/30788497/)
3. Wang D, Zhu X, Siqin B, Ren C, Yi F. Long non-coding RNA CYTOR modulates cancer progression through miR-136-5p/MAT2B axis in renal cell carcinoma. *Toxicol Appl Pharmacol.* 2022; 447:116067. <https://doi.org/10.1016/j.taap.2022.116067> PMID:[35597301](https://pubmed.ncbi.nlm.nih.gov/35597301/)
4. Patel DN, Figlin RA, Kim HL. Adjuvant treatment for renal cell carcinoma: do we finally have a major breakthrough? *Clin Adv Hematol Oncol.* 2016; 14:907–14. PMID:[27930642](https://pubmed.ncbi.nlm.nih.gov/27930642/)
5. Li A, Cao C, Gan Y, Wang X, Wu T, Zhang Q, Liu Y, Yao L, Zhang Q. ZNF677 suppresses renal cell carcinoma progression through N6-methyladenosine and transcriptional repression of CDKN3. *Clin Transl Med.* 2022; 12:e906. <https://doi.org/10.1002/ctm2.906> PMID:[35678231](https://pubmed.ncbi.nlm.nih.gov/35678231/)
6. Nachtergaele S, He C. Chemical Modifications in the Life of an mRNA Transcript. *Annu Rev Genet.* 2018; 52:349–72. <https://doi.org/10.1146/annurev-genet-120417-031522> PMID:[30230927](https://pubmed.ncbi.nlm.nih.gov/30230927/)

7. Wu G, Yu AT, Kantartzis A, Yu YT. Functions and mechanisms of spliceosomal small nuclear RNA pseudouridylation. *Wiley Interdiscip Rev RNA*. 2011; 2:571–81.  
<https://doi.org/10.1002/wrna.77>  
PMID:[21957045](https://pubmed.ncbi.nlm.nih.gov/21957045/)
8. Charette M, Gray MW. Pseudouridine in RNA: what, where, how, and why. *IUBMB Life*. 2000; 49:341–51.  
<https://doi.org/10.1080/152165400410182>  
PMID:[10902565](https://pubmed.ncbi.nlm.nih.gov/10902565/)
9. Li X, Ma S, Yi C. Pseudouridine: the fifth RNA nucleotide with renewed interests. *Curr Opin Chem Biol*. 2016; 33:108–16.  
<https://doi.org/10.1016/j.cbpa.2016.06.014>  
PMID:[27348156](https://pubmed.ncbi.nlm.nih.gov/27348156/)
10. Xue C, Chu Q, Zheng Q, Jiang S, Bao Z, Su Y, Lu J, Li L. Role of main RNA modifications in cancer: N<sup>6</sup>-methyladenosine, 5-methylcytosine, and pseudouridine. *Signal Transduct Target Ther*. 2022; 7:142.  
<https://doi.org/10.1038/s41392-022-01003-0>  
PMID:[35484099](https://pubmed.ncbi.nlm.nih.gov/35484099/)
11. Cerneckis J, Cui Q, He C, Yi C, Shi Y. Decoding pseudouridine: an emerging target for therapeutic development. *Trends Pharmacol Sci*. 2022; 43:522–35.  
<https://doi.org/10.1016/j.tips.2022.03.008>  
PMID:[35461717](https://pubmed.ncbi.nlm.nih.gov/35461717/)
12. Martinez NM, Su A, Burns MC, Nussbacher JK, Schaening C, Sathe S, Yeo GW, Gilbert WV. Pseudouridine synthases modify human pre-mRNA co-transcriptionally and affect pre-mRNA processing. *Mol Cell*. 2022; 82:645–59.e9.  
<https://doi.org/10.1016/j.molcel.2021.12.023>  
PMID:[35051350](https://pubmed.ncbi.nlm.nih.gov/35051350/)
13. Fitzek E, Joardar A, Gupta R, Geisler M. Evolution of Eukaryal and Archaeal Pseudouridine Synthase Pus10. *J Mol Evol*. 2018; 86:77–89.  
<https://doi.org/10.1007/s00239-018-9827-y>  
PMID:[29349599](https://pubmed.ncbi.nlm.nih.gov/29349599/)
14. Penzo M, Guerrieri AN, Zacchini F, Treré D, Montanaro L. RNA Pseudouridylation in Physiology and Medicine: For Better and for Worse. *Genes (Basel)*. 2017; 8:301.  
<https://doi.org/10.3390/genes8110301>  
PMID:[29104216](https://pubmed.ncbi.nlm.nih.gov/29104216/)
15. Guzzi N, Cieśła M, Ngoc PCT, Lang S, Arora S, Dimitriou M, Pimková K, Sommarin MNE, Munita R, Lubas M, Lim Y, Okuyama K, Soneji S, et al. Pseudouridylation of tRNA-Derived Fragments Steers Translational Control in Stem Cells. *Cell*. 2018; 173:1204–16.e26.  
<https://doi.org/10.1016/j.cell.2018.03.008>  
PMID:[29628141](https://pubmed.ncbi.nlm.nih.gov/29628141/)
16. Fang Z, Shen HY, Xu Q, Zhou HL, Li L, Yang SY, Zhu Z, Tang JH. PUS1 is a novel biomarker for predicting poor outcomes and triple-negative status in breast cancer. *Front Oncol*. 2022; 12:1030571.  
<https://doi.org/10.3389/fonc.2022.1030571>  
PMID:[36457503](https://pubmed.ncbi.nlm.nih.gov/36457503/)
17. Jin M, Xu Q, Li J, Xu S, Tang C. Micro-RNAs in Human Placenta: Tiny Molecules, Immense Power. *Molecules*. 2022; 27:5943.  
<https://doi.org/10.3390/molecules27185943>  
PMID:[36144676](https://pubmed.ncbi.nlm.nih.gov/36144676/)
18. Fernandez-Vizarra E, Berardinelli A, Valente L, Tiranti V, Zeviani M. Nonsense mutation in pseudouridylate synthase 1 (PUS1) in two brothers affected by myopathy, lactic acidosis and sideroblastic anaemia (MLASA). *J Med Genet*. 2007; 44:173–80.  
<https://doi.org/10.1136/jmg.2006.045252>  
PMID:[17056637](https://pubmed.ncbi.nlm.nih.gov/17056637/)
19. Cao M, Donà M, Valentino ML, Valentino L, Semplicini C, Maresca A, Cassina M, Torracco A, Galletta E, Manfioli V, Sorarù G, Carelli V, Stramare R, et al. Clinical and molecular study in a long-surviving patient with MLASA syndrome due to novel PUS1 mutations. *Neurogenetics*. 2016; 17:65–70.  
<https://doi.org/10.1007/s10048-015-0465-x>  
PMID:[26556812](https://pubmed.ncbi.nlm.nih.gov/26556812/)
20. Zhang MM, Jia Y, Li P, Qiao Y, Han KL. New Protocol-Guided Exploitation of a Lysosomal Sulfatase Inhibitor to Suppress Cell Growth in Glioblastoma Multiforme. *J Med Chem*. 2021; 64:8599–606.  
<https://doi.org/10.1021/acs.jmedchem.1c00559>  
PMID:[34096701](https://pubmed.ncbi.nlm.nih.gov/34096701/)
21. Xu W, Tao J, Zhu W, Liu W, Anwaier A, Tian X, Su J, Shi G, Huang H, Wei G, Li C, Qu Y, Zhang H, Ye D. Comprehensive Multi-Omics Identification of Interferon-γ Response Characteristics Reveals That RBCK1 Regulates the Immunosuppressive Microenvironment of Renal Cell Carcinoma. *Front Immunol*. 2021; 12:734646.  
<https://doi.org/10.3389/fimmu.2021.734646>  
PMID:[34795663](https://pubmed.ncbi.nlm.nih.gov/34795663/)
22. Tang C, Li L, Xu Q, Xu S, Lin C, Cao B. ACKR3 orchestrates Hedgehog signaling to promote renal cell carcinoma progression. *Mol Carcinog*. 2023; 62:882–93.  
<https://doi.org/10.1002/mc.23532>  
PMID:[36988340](https://pubmed.ncbi.nlm.nih.gov/36988340/)
23. Zhu H, Ren Q, Yan Z, Xu S, Luo J, Wu X, Tang C. Human HAND1 inhibits the conversion of cholesterol to steroids in trophoblasts. *J Genet Genomics*. 2022; 49:350–63.

- <https://doi.org/10.1016/j.jgg.2021.07.014>  
PMID:34391879
24. Jin M, Xu S, Cao B, Xu Q, Yan Z, Ren Q, Lin C, Tang C. Regulator of G protein signaling 2 is inhibited by hypoxia-inducible factor-1 $\alpha$ /E1A binding protein P300 complex upon hypoxia in human preeclampsia. *Int J Biochem Cell Biol.* 2022; 147:106211.  
<https://doi.org/10.1016/j.biocel.2022.106211>  
PMID:35430356
25. Tang C, Wu X, Ren Q, Yao M, Xu S, Yan Z. Hedgehog signaling is controlled by Rac1 activity. *Theranostics.* 2022; 12:1303–20.  
<https://doi.org/10.7150/thno.67702>  
PMID:35154488
26. Li L, Zhu C, Xu Q, Xu S, Ye J, Xu D, Wang L, Gan S, Liu B, Tang C. ALKBH1 contributes to renal cell carcinoma progression by reducing N6-methyladenine of GPR137. *Eur J Clin Invest.* 2023; e13986.  
<https://doi.org/10.1111/eci.13986>  
PMID:36920340
27. Jin M, Cao B, Lin C, Li J, Xu Q, Ren Q, Xu S, Tang C. Tianma Gouteng Decoction Exerts Pregnancy-Protective Effects Against Preeclampsia *via* Regulation of Oxidative Stress and NO Signaling. *Front Pharmacol.* 2022; 13:849074.  
<https://doi.org/10.3389/fphar.2022.849074>  
PMID:35401241
28. Jin M, Xu S, Li J, Li L, Tang C. Role of ARID1A in the Regulation of Human Trophoblast Migration and Invasion. *Reprod Sci.* 2022; 29:2363–73.  
<https://doi.org/10.1007/s43032-021-00686-0>  
PMID:34255312
29. Tang C, Takahashi-Kanemitsu A, Kikuchi I, Ben C, Hatakeyama M. Transcriptional Co-activator Functions of YAP and TAZ Are Inversely Regulated by Tyrosine Phosphorylation Status of Parafibromin. *iScience.* 2018; 1:1–15.  
<https://doi.org/10.1016/j.isci.2018.01.003>  
PMID:30227954
30. Frye M, Harada BT, Behm M, He C. RNA modifications modulate gene expression during development. *Science.* 2018; 361:1346–9.  
<https://doi.org/10.1126/science.aau1646>  
PMID:30262497
31. Cui Q, Yin K, Zhang X, Ye P, Chen X, Chao J, Meng H, Wei J, Roeth D, Li L, Qin Y, Sun G, Zhang M, et al. Targeting PUS7 suppresses tRNA pseudouridylation and glioblastoma tumorigenesis. *Nat Cancer.* 2021; 2:932–49.  
<https://doi.org/10.1038/s43018-021-00238-0>  
PMID:35121864
32. Waalkes TP, Dinsmore SR, Mrochek JE. Urinary excretion by cancer patients of the nucleosides N-dimethylguanosine, 1-methylinosine, and pseudouridine. *J Natl Cancer Inst.* 1973; 51:271–4.  
<https://doi.org/10.1093/jnci/51.1.271>  
PMID:4720877
33. Seidel A, Brunner S, Seidel P, Fritz GI, Herbarth O. Modified nucleosides: an accurate tumour marker for clinical diagnosis of cancer, early detection and therapy control. *Br J Cancer.* 2006; 94:1726–33.  
<https://doi.org/10.1038/sj.bjc.6603164>  
PMID:16685264
34. Song D, Guo M, Xu S, Song X, Bai B, Li Z, Chen J, An Y, Nie Y, Wu K, Wang S, Zhao Q. HSP90-dependent PUS7 overexpression facilitates the metastasis of colorectal cancer cells by regulating LASP1 abundance. *J Exp Clin Cancer Res.* 2021; 40:170.  
<https://doi.org/10.1186/s13046-021-01951-5>  
PMID:33990203
35. Li H, Chen L, Han Y, Zhang F, Wang Y, Han Y, Wang Y, Wang Q, Guo X. The Identification of RNA Modification Gene *PUS7* as a Potential Biomarker of Ovarian Cancer. *Biology (Basel).* 2021; 10:1130.  
<https://doi.org/10.3390/biology10111130>  
PMID:34827123
36. Shen S, Faouzi S, Bastide A, Martineau S, Malka-Mahieu H, Fu Y, Sun X, Mateus C, Routier E, Roy S, Desaubry L, André F, Eggermont A, et al. An epitranscriptomic mechanism underlies selective mRNA translation remodelling in melanoma persister cells. *Nat Commun.* 2019; 10:5713.  
<https://doi.org/10.1038/s41467-019-13360-6>  
PMID:31844050

# SUPPLEMENTARY MATERIALS

## Supplementary Figure



Supplementary Figure 1. Data of *PUS1* mRNA expression analysis in 33 renal cancer cell lines from the CCLE portal.